Available online at www.sciencedirect.com
SCIENCE DIRECT®
Polymer 44 (2003) 4959–4967
polymer
www.elsevier.com/locate/polymer

Control of structure, morphology and property in electrospun poly(glycolide-*co*-lactide) non-woven membranes via post-draw treatments

Xinhua Zong[a], Shaofeng Ran[a], Dufei Fang[b], Benjamin S. Hsiao[a,*], Benjamin Chu[a,*]

[a]*Department of Chemistry, State University of New York at Stony Brook, Stony Brook, NY 11794-3400, USA*
[b]*Stonybrook Technology and Applied Research, Inc., P.O. Box 1336, Stony Brook, NY 11790, USA*

Received 26 February 2003; received in revised form 15 May 2003; accepted 21 May 2003

Abstract

Non-woven biodegradable membranes fabricated by electrospinning have recently attracted a great deal of attention for biomedical applications. In this study, microstructure, morphology and texture of electrospun poly(glycolide-*co*-lactide) (GA/LA: 90:10, PLA10GA90) non-woven membranes were investigated after post-draw and thermal treatments to tailor the degradation and mechanical properties. As-prepared electrospun PLA10GA90 membranes exhibited a low degree of crystallinity. When annealed at elevated temperatures without drawing, the membrane showed a higher degree of crystallinity with distinct lamellar structure but no overall orientation. The crystal orientation improved significantly when the membrane was drawn and annealed. As the elongation ratio increased, the degree of orientation and the tensile strength were increased. The corresponding tensile retention time was also increased from 2 to 12 days during in vitro degradation. Post-drawn and annealed membranes exhibited a slower degradation rate in the beginning of incubation, but a faster rate after two weeks of degradation when compared to as-spun membranes.

Keywords: Poly(glycolide-*co*-lactide); Drawing; Electrospun membrane

1. Introduction

Synthetic biodegradable poly(lactide)- and poly(glycolide)-based polymers (PLGA) are routinely used in medical and biological applications such as medical implants (e.g. sutures), scaffolds for tissue engineering and drug delivery devices. The applications require materials with well-defined properties and functionality. In many situations, the most important properties are the biocompatibility, mechanical performance and degradation rate. The issues of biocompatibility and degradation rate in PLGA polymers have been well investigated in the literature, but the requirements for mechanical properties vary substantially. Typically desired mechanical properties of medical implants involve not only adequate initial tensile strength and modulus, but also sufficient retention of tensile strength during in vitro or in vivo degradation. In the latter, the rate at which the mechanical properties are reduced is particularly important for the success of some applications.

The mechanical properties of PLGA polymers in the form of fibers, films and injection-molded parts are influenced not only by their chemical compositions, but also by their crystalline structure and morphology, such as crystallinity and crystalline orientation. Many investigations have been carried out to study the effects of structure and morphology on the physico–mechanical properties of PLGA polymers in medical applications [1–6]. Several reports have particularly dealt with the subject of structure and property relationship for PLGA-based fibers [7–9]. For example, Fredericks et al. reported that the tensile strength of PLGA polymers relied on the tie molecules in the amorphous region [7]. Ginde et al. demonstrated that heat-treated PGA fibers were stronger than the un-treated ones [8]. They also discovered that the tensile strength declined in the PGA fibers during in vitro degradation, which was independent of the fiber diameter. Tsuji and Ikada pointed out that the poor initial mechanical property of the amorphous polymers could be improved by forcing the

* Tel.: +1-631-632-7929; fax: +1-631-632-6518.
E-mail addresses: bhsiao@notes.cc.sunysb.edu (B.S. Hsiao), bchu@notes.cc.sunysb.edu (B. Chu).

0032-3861/03/$ - see front matter © 2003 Elsevier Science Ltd. All rights reserved.
doi:10.1016/S0032-3861(03)00464-6

chains to align along the mechanical direction [9]. Usually, the amorphous distribution in the semi-crystalline polymer played an important role in the retention time of tensile strength, whereby a higher degree of crystallinity and a higher molecular orientation often resulted in higher values of the tensile strength and longer degradation times. There were also several studies that investigated the relationships among processing, structure and property of PLGA fibers [10–12]. It was shown that the most effective means to improve the degree of polymer orientation and crystallinity of PLGA fibers, and hence the mechanical and degradation properties, was the post-treatment method involving mechanical drawing at elevated temperatures.

Recently, there has been a tremendous growth of research activities to explore the technology of electrospinning to fabricate non-woven fibrous membranes. The majority of the studies are related to the generation of new nanostructured materials and their applications. Among them, a large fraction of studies were intended for biomedical applications, such as substrates for tissue regeneration, immobilized enzymes and catalyst systems, wound dressing articles, artificial blood vessels and materials for the prevention of post-operative induced adhesions [13–21]. As mentioned earlier, the successful implementation of electrospun membranes for biomedical applications often involves the control of mechanical and biodegradation properties. The objectives of this study thus were two-fold: (1) to examine several post-treatment techniques to manipulate the mechanical and degradation properties of electrospun membranes, (2) to understand the relationship among the property, structure and morphology of the fiber, as well as the texture of the electrospun membrane. The post-treatment methods included the sequentially applied uniaxial drawing and annealing process. The structure and morphology changes under different post-treatment conditions have been investigated by synchrotron wide-angle X-ray diffraction (WAXD) and small-angle X-ray scattering (SAXS) techniques. The effects of structure and morphology changes in the fibers on the in vitro degradation properties, such as degradation rate and mechanical properties have also been investigated.

2. Experimental

2.1. Materials and preparation

The chosen PLGA sample was a poly(glycolide-*co*-lactide) random copolymer produced by Ethicon Inc. This copolymer contained 90 mol% of glycolic acid and 10 mol% of L-lactic acid (PLA10GA90), and exhibited an intrinsic viscosity of 1.56 dL/g in 0.1 g/ml hexafluoroisopropanol (HFIP, Aldrich) at room temperature. The sample had a weight average molecular weight (M_w) of approximately 7.5×10^4 g/mol and a polydispersity index of 3.1. HFIP was used to dissolve PLA10GA90 for the electrospinning process. This sample was semi-crystalline with a typical degree of crystallinity of 40%. The nominal melting temperature of the PGA crystal in PLA10GA90 was 201 °C, and the glass transition temperature of the quenched amorphous PLA10GA90 sample was 42 °C.

Detailed electrospinning processing conditions were published elsewhere [17]. In this study, typical electrospinning parameters were as follows. The electric field strength was 2 kV/cm (the distance between the spinneret and the ground was 15 cm). The solution feed rate per spinneret was 100 μl/min. The membranes were electrospun from different concentrations of PLA10GA90 solutions in HFIP under an electric field of 30 kV.

2.2. Membrane post-treatment processes

A modified Instron 4400 tensile stretching apparatus with a custom-built heating chamber was used to post-treat the electrospun PLA10GA90 membranes as well as to characterize their mechanical properties. In situ synchrotron X-ray studies were carried out simultaneously during post-treatment processing (deformation and crystallization) to monitor the structure and morphology changes. The modification of the Instron apparatus allowed the sample to be stretched symmetrically along the uniaxial direction, which also assured that the focused X-ray beam always illuminated the same position on the sample during stretching. All electrospun PLA10GA90 membranes for the post-treatment process were cut into a rectangular shape with dimensions of $20 \times 5 \times 0.2\ mm^3$. The length and width of samples were measured with a ruler having the precision of 1 mm (ca. 5%), and the thickness of samples were measured with a digital micrometer having the precision of 1 μm (ca. 5%). The post-treatments involved two processes: uniaxial drawing and annealing, using the following procedures.

(1) The membranes were drawn to different desired extension ratios at a constant rate of 4 mm/min at room temperature (for the mechanical property testing, the sample was stretched to break at room temperature).
(2) The stretched membranes were subsequently heated to four different temperatures (60, 70, 80 and 90 °C) at a rate of 5 °C/min under a constant strain for annealing.

The stress–strain curves were recorded automatically during the drawing and annealing processes.

2.3. In situ synchrotron X-ray characterization techniques

The tensile stretching apparatus was adapted to a three-pinhole X-ray collimation facility at the X3A2 beamline ($\lambda = 1.54$ Å) of the National Synchrotron Light Source (NSLS), Brookhaven National Laboratory (BNL) to per-

form the in situ synchrotron X-ray studies. Two-dimensional (2D) WAXD and SAXS patterns were collected separately using the CCD X-ray detector (MARUSA) during both drawing and annealing processes. The distance from the CCD detector to the sample was 114.1 mm for the WAXD study and 1370 mm for the SAXS study, respectively. The typical data acquisition time for each X-ray image was 30 s. The diffraction angle in WAXD was calibrated by using an Al_2O_3 standard, and the scattering angle in SAXS was calibrated by using a silver behnate standard. All images were corrected for fluctuations of the synchrotron beam intensity, the sample volume change, and beam absorption.

2.4. In vitro degradation study of electrospun non-woven membranes

As-spun and post-treated electrospun PLA10GA90 membranes were cut into a rectangular shape with dimensions of $20 \times 2 \times 0.2$ mm^3 for in vitro degradation studies. The cut specimens were placed in closed bottles containing phosphate buffer solution (PBS, the pH value was 7.26 ± 0.04) and incubated in vitro at a temperature of 37.0 ± 0.1 °C for different periods of time. Three specimens were recovered at the end of each degradation period and were weighed accordingly after having been dried in a vacuum oven at room temperature for one week. The mass loss of each sample was calculated, based on the initial mass of the sample before incubation.

3. Results and discussion

3.1. Structure and mechanical properties of as-prepared electrospun PLA10GA90 membranes

Fig. 1 shows morphological changes of as-prepared electrospun PLA10GA90 membranes as a function of PLA10GA90 concentration in HFIP. The membrane electrospun from a concentration of 7.5 wt% exhibited a beads-on-string structure (Fig. 1(A)), while both 10 and 15 wt% of PLA10GA90 formed a fibrous structure. In addition, the diameter of the fibers increased with increasing concentration with an average diameter of around 400 nm and 1 μm for fibers electrospun from 10 and 15 wt%, respectively. This phenomenon has been observed by us earlier [17] and can be understood by the following explanation. At lower concentrations, electrospun fibers are harder to dry before they reach the collection plate. As the wet fibers must undergo a solidification process under the influence of surface tension and chain relaxation processes due to the viscoelastic property of viscous polymer solutions, this process would result in the undulating morphology as shown in Fig. 1(A). In contrast, at higher concentrations, the electrospun fibers are mostly dried by the time they reach the collection plate. As a result,

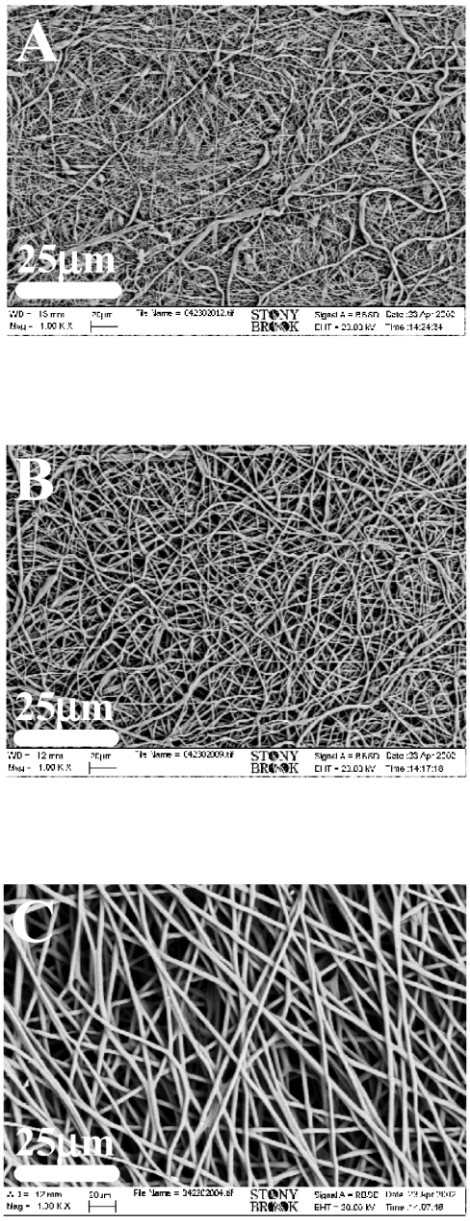

Fig. 1. SEM images of PLA10GA90 membranes electrospun under 2 kV/cm electric field strength, at a feed rate of 100 μl/min and different concentrations: (A) 7.5 wt%; (B) 10 wt%; and (C) 15 wt% in HFIP.

the uniform fiber morphology is obtained (Fig. 1(B) and (C)). However, as the solution becomes more viscous, the diameter of the electrospun fiber becomes greater as the degree of polymer extension is lower.

The variations of structure and morphology in these electrospun membranes resulted in very different mechanical properties, which are shown in Fig. 2. In this figure, the nominal stress–strain curves are illustrated for different samples having the same dimensions (including the thickness). The stress at break and the initial modulus for each sample are summarized in Table 1. The membrane electrospun from 7.5 wt% PLA10GA90 solution was very weak with the stress at break (τ) of around 2.5 MPa and the

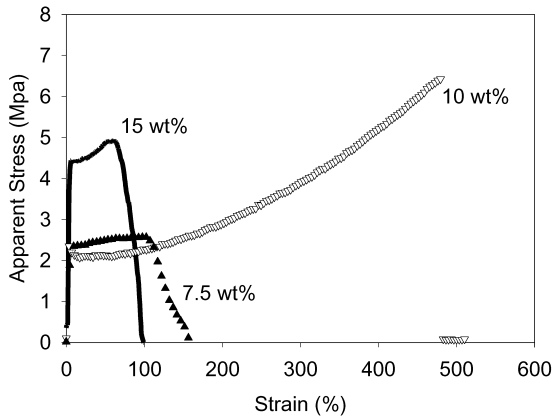

Fig. 2. Stress–strain curves for PLA10GA90 electrospun membranes prepared under the 2 kV/cm electric field, at a feed rate of 100 μl/min and different concentrations of 7.5, 10 and 15 wt%, respectively.

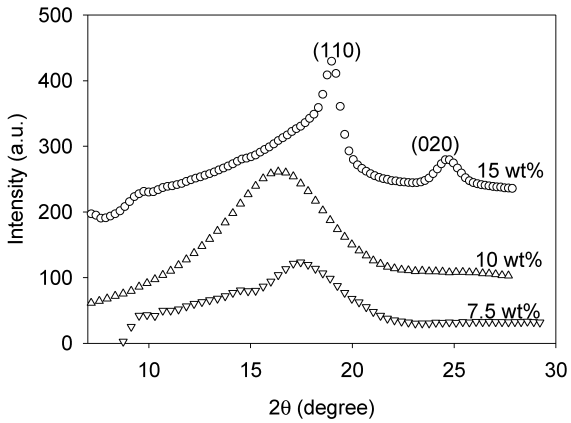

Fig. 3. Diffraction profiles extracted from 2D WAXD patterns of electrospun membranes at different concentrations of 7.5, 10 and 15 wt% in HFIP, respectively.

strain at break (ε) of around 110%. In contrast, the membrane electrospun from 15 wt% solution exhibited a higher value of stress at break (4.9 MPa) but a lower value of the strain at break (60%). The membrane electrospun from 10 wt% solution exhibited the optimum mechanical properties with stress at break of around 6.0 MPa and an extremely high ultimate strain value around of 490% due to the uniform fiber diameter (400 nm) with essentially no crystalline structure. The stronger stress at break value but lower strain at break value for the membrane electrospun from 15 wt% PLA10GA90 solution were due to its larger diameter and the partially crystalline structure, which will be discussed later. The semi-crystalline structure in the 15 wt% membrane enhanced the tensile strength but decreased the elongation at break value.

As reported by us and the other group earlier [17,22] that electrospinning retards the crystallization process of semi-crystalline polymers. The similar behavior was also observed in electrospinning of PLA10GA90 membranes. Fig. 3 shows the WAXD profiles of PLA10GA90 membranes electrospun from different concentrations in HFIP. The membranes formed from lower concentrations (7.5 and 10 wt%) exhibited only amorphous peaks, while the membrane electrospun from 15 wt% showed two crystalline peaks having an intermediate degree of crystallinity of around 30% (melt spun PLA10GA90 suture fibers usually have a crystallinity of around 55%). These findings again confirmed that crystallization was retarded during electrospinning, which could be attributed to the rapid solidification of the stretched chains at high elongational rates during the later stages of electrospinning that significantly hindered the formation of crystals. In other words, the stretched chains did not have enough time to organize into 3D ordered crystal structures before they were solidified. Although the membrane electrospun from 15 wt% PLA10GA90/HFIP solution showed an intermediate level of crystallinity (30%), the retardation effect on crystallization due to rapid solidification of the stretched chains was still present. However, as the fibers had a larger diameter (Fig. 1), the polymer chains probably had sufficient time to organize themselves into suitable crystal structures.

Table 1
Mechanical properties of PLA10GA90 membranes electrospun from different concentrations in HFIP (values given are averaged from 3 samples for each concentration)

Concentration (wt%)	E (MPa)	YS (MPa)	τ (MPa)	ε (%)
15	87 ± 11	4.3 ± 0.9	4.9 ± 0.5	60 ± 11
10	71 ± 7	2.5 ± 0.1	6.0 ± 0.2	490 ± 25
7.5	42 ± 3	2.3 ± 0.2	2.5 ± 0.5	110 ± 20

E, Young's modulus; YS, yield stress; τ, ultimate stress; ε, ultimate strain.

3.2. Structure and morphology of post-treated electrospun membranes

As the electrospun membranes from 10 wt% of PLA10-GA90/HFIP solution exhibited the optimum mechanical properties, we used these membranes as the base materials for post-treatments to enhance the mechanical properties. The post-treatment conditions were described earlier. All membranes were first stretched to a desired strain at room temperature, and then subsequently annealed and crystallized at different elevated temperatures in the environmental chamber.

3.2.1. Texture observations

Fig. 4(A) shows the SEM images of the membranes electrospun from the 10 wt% PLA10GA90/HFIP solution. After being stretched with a strain of 300% at a constant rate and subsequently crystallized at 90 °C for 20 min, the post-treated electrospun PLA10GA90 membrane is shown in Fig. 4(B). A completely different texture was seen in the drawn and annealed membrane, where all the fibers were aligned along the stretching direction and the fiber diameters were decreased. In addition, the porosity of the membrane also decreased slightly, but the pore size

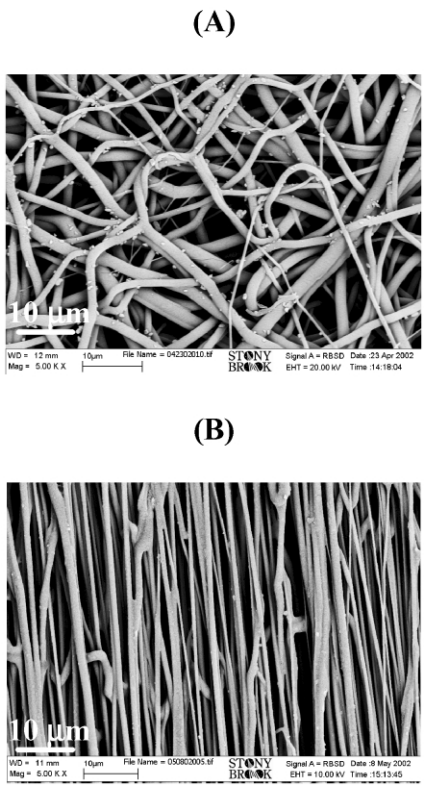

Fig. 4. SEM images of (A) as-prepared electrospun PLA10GA90 membranes from 10 wt% in HFIP and (B) the same one annealed at 90 °C for 20 min under a constant deformation strain of 450%.

distribution became very uniform. The density and porosity of the as-prepared electrospun PLA10GA90 membrane and the post-treated membrane are summarized in Table 2. It is seen that the density of the as-prepared membrane (0.44 g/cm^3) increased to 0.52 g/cm^3 after drawn and annealed treatments, while the porosity of the membrane (porosity $= (1 - \rho/\rho_0) \times 100$, where ρ is the density of electrospun membrane calculated from an average of three samples using the mass divided by the volume of the sample [25]; ρ_0 is the initial raw pallet density) decreased from 71 to 65%.

3.2.2. Crystalline structure by WAXD

2D WAXD patterns of the PLA10GA90 membranes (electrospun from 10 wt% HFIP solution) crystallized at 60 °C without deformation and under a constant strain of 250% are shown in Fig. 5(A) and (B), respectively. These images were corrected for air scattering and instrumental background. The crystallization times were 20 min for both samples. The isotropic scattering feature in Fig. 5(A) indicated that the electrospun PLA10GA90 membrane was still amorphous even when the sample was annealed at a temperature well above its glass transition temperature (38 °C) for 20 min. In contrast, two distinct oriented crystal reflection peaks were found in the drawn and annealed membrane (Fig. 5(B)). These two peaks can be indexed as (110) and (020) reflections from the orthorhombic unit cell ($a = 5.22$ Å, $b = 6.19$ Å, $c = 7.02$ Å) of the pure PGA crystals [23]. It was evident that the crystallization rate of electrospun PLA10GA90 membrane was significantly increased by the deformation process, where the oriented chains facilitated the crystallization process.

Fig. 6 shows the WAXD patterns of the electrospun PLA10GA90 membrane annealed at 90 °C for 20 min under different strains. The relative intensities of diffraction peaks along the equatorial direction were found to substantially increase with increasing strain. This was expected as the polymer chains were aligned better along the stretching direction with the increase in strain. The evolution of the two reflection peaks (110) and (020) indicated that the

Table 2
Comparison of density and porosity of the as-prepared and post-treated membranes electrospun from 10 wt% PLA10GA90 in HFIP (values given are averaged from 15 samples for in vitro degradation study). The post-treatments involved the tensile stretching to a strain of 300% and subsequent crystallization at 90 °C for 20 min

Sample	Density (g/cm^3)	Porosity (%)[a]
As-prepared PLA10GA90	0.44 ± 0.05	71
Drawn/Annealed PLA10GA90	0.52 ± 0.04	65

[a] *Porosity* $= (1 - \rho/\rho_0) \times 100$; ρ, density of electrospun membrane; ρ_0, initial raw pallet density (1.49 g/cm^3).

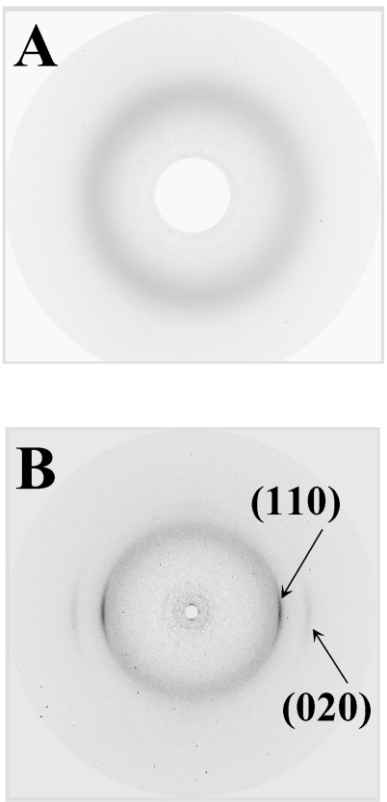

Fig. 5. Comparison of 2D WAXD patterns of electrospun PLA10GA90 membranes from 10 wt% solution: (A) membrane crystallized at 60 °C without stretching; (B) membrane crystallized at 60 °C under a strain of 250%.

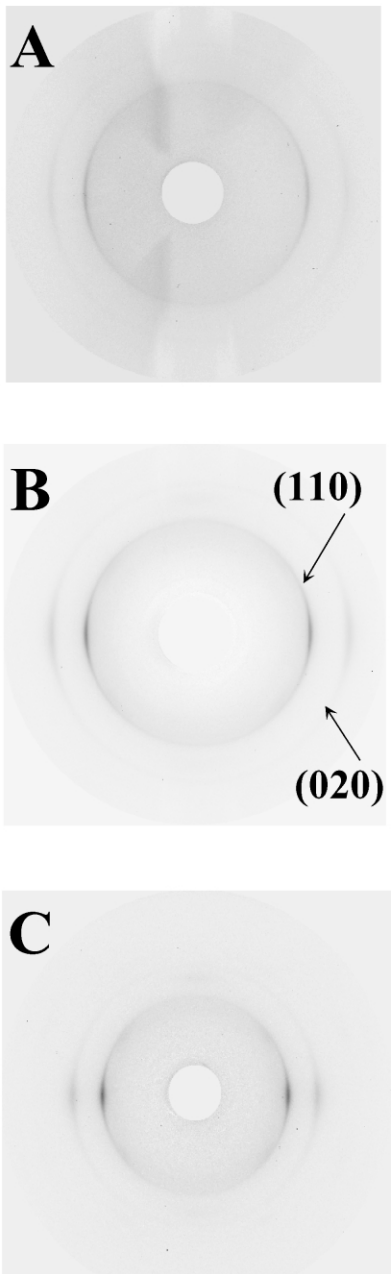

Fig. 6. WAXD patterns of electrospun PLA10GA90 (prepared from 10 wt% solution) annealed under 90 °C for 20 min under strains of (A) 150%; (B) 300%; and (C) 450%.

degree of crystallinity and crystal orientation all increased with the increase in the deformation strain.

Next, we will discuss the effect of annealing temperature under the same deformation conditions. The crystallization results from the drawn and annealed samples prepared under a constant strain (300%) are listed in Table 3. Each sample was drawn to the same strain (300%) and then annealed at different temperatures for 20 min. Table 3 shows that the crystallinity increased from 23% at 70 °C to 40% at 90 °C. Since the fastest crystallization rate of the bulk PLA10GA90 resin was around the temperature of 95 °C, the crystallinity of electrospun PLA10GA90 membrane

Table 3
Degree of crystallinity and orientation for electrospun PLA10GA90 from 10 wt% solution annealed at different temperatures under the same deformation strain of 300%

	Temperature (°C)		
	70	80	90
Crystallinity (%)	23	30	40
Crystal orientation (f_2 of 110 peak)	−0.22	−0.17	−0.08

f_2, Herman's orientation function (f_2 is −0.5 for perfect crystal orientation along the stretching direction, and 1/3 for random orientation).

increased with crystallization temperature in the chosen range (60–90 °C). Meanwhile, the degree of crystal orientation within the stretched membrane was found to decrease with increasing crystallization temperature. In Table 3, it is seen that the Herman's orientation function f_2 of the (110) reflection peak was closer to −0.5 when the annealing temperature was the lowest (we note that for perfect crystal orientation along the stretching direction f_2 of the (110) peak is −0.5; while f_2 is 1/3 for random orientation). The decrease in crystal orientation was due to the rapid relaxation of amorphous chains by the crystallization process of adjacent chains. In other words, when crystallization took place, the initial stress around the extended amorphous chains was decreased, resulting in the loss of crystal orientation. As more crystallization occurred at higher temperatures, a larger fraction of crystal orientation was lost.

3.2.3. Lamellar structure by SAXS

Fig. 7 shows typical 2D SAXS patterns of electrospun PLA10GA90 membranes (from 10 wt% solution) crystallized at 90 °C without deformation (Fig. 7(A)) and under the strain of 450% for 20 min (Fig. 7(B)). Fig. 7(A) shows that the typical lamellar structure with a weak orientation was formed in the annealed membrane without deformation. In contrast, the SAXS pattern of the drawn and annealed membrane exhibited a very strong streak along the equator and two sharp spots on the meridian (Fig. 7(B)). The interpretation of the equatorial streak was more complicated since it might contain several contributions including the microfibril structure from the crystal, the needle-shaped microvoid morphology and the surface reflection/scattering of the fibers. In our case, we believe that the needle-shaped microvoids formed after stretching could be the main contribution to the formation of the equatorial streak [24]. The two-spot pattern with the scattering maxima on the meridian indicated that the drawn and annealed fiber contained a distinct crystalline/amorphous lamellar structure with excellent orientation. In this morphology, the polymer chains were aligned along the stretching direction with a high degree of orientation, where the lamellae were perpendicular to the fiber axis (or draw axis).

3.2.4. Mechanical property evaluation

The mechanical properties of the as-prepared

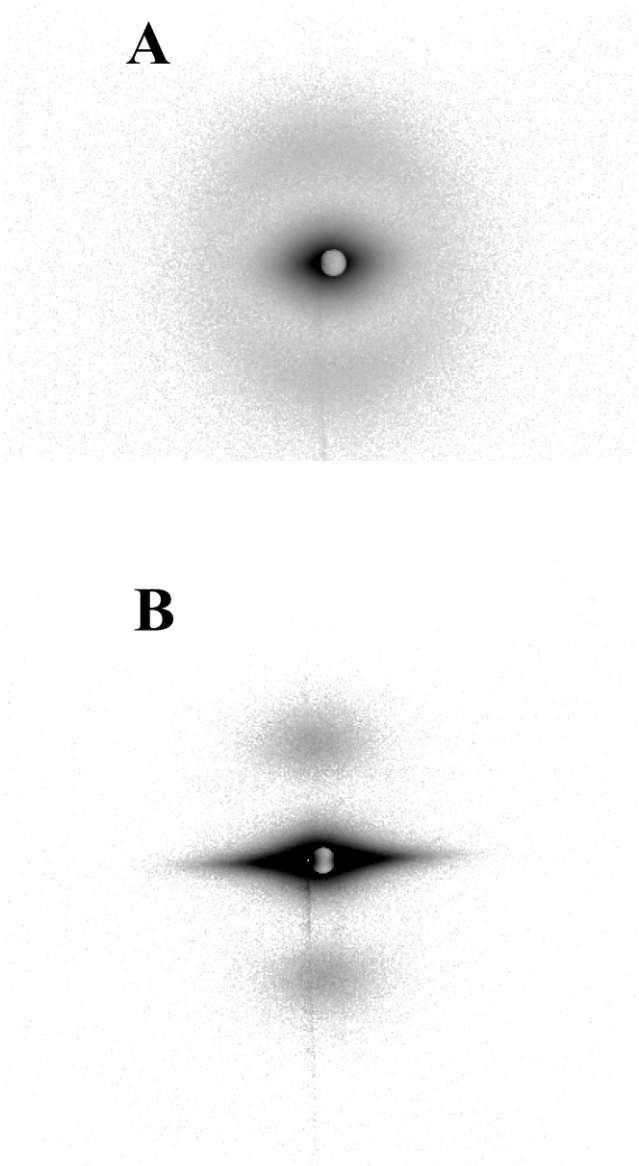

Fig. 7. SAXS patterns of electrospun PLA10GA90 membrane crystallized at 90 °C (A) without deformation and (B) with a strain of 450% for 20 min.

PLA10GA90 membrane and the membrane annealed under a constant strain of 450% at 90 °C for 20 min were compared, with the corresponding stress–strain curves being shown in Fig. 8. The value of tensile strength at break was found to increase by eight times after annealing under a strain of 450%. However, the elongation at break of the post-treated membrane in the stretching direction of post treatment was found to decrease significantly. In other words, the membrane became much stronger but relatively brittle after the stretching and annealing treatments, which could be attributed to the increase in the degree of crystallinity and orientation after drawing and annealing processes. More importantly, the retention time of tensile strength for the post-treated membranes during in vitro

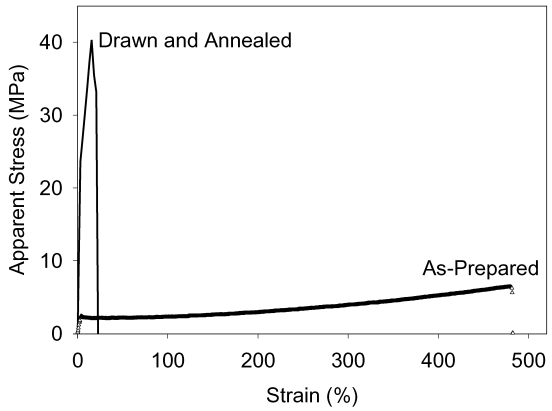

Fig. 8. Mechanical property comparison between the as-prepared electrospun PLA10GA90 membrane with that annealed at 90 °C for 20 min under a strain of 450%.

degradation had been greatly improved, which will be discussed next.

3.2.5. In vitro degradation properties

The PLA10GA90 membranes electrospun from 10 wt% in HFIP were annealed at 90 °C for 20 min under a constant strain of 300% for in vitro degradation studies. Fig. 9 shows the changes in mechanical properties of these samples during in vitro degradation. The mechanical properties of post-treated membranes were totally different from those of untreated ones. The as-prepared electrospun PLA10GA90 lost its mechanical strength within two days of degradation. In fact no data could be obtained to evaluate the strength retention property during degradation of the as-prepared membranes. For post-treated PLA10GA90 membranes, reasonable (weak but identifiable) tensile strength retention time was prolonged to more than eight days. During the first six days of degradation, the shape of the stress–strain curves was maintained as that of the initially treated sample. A prolonged plastic flow region before the stress rise was found, which could be attributed to the

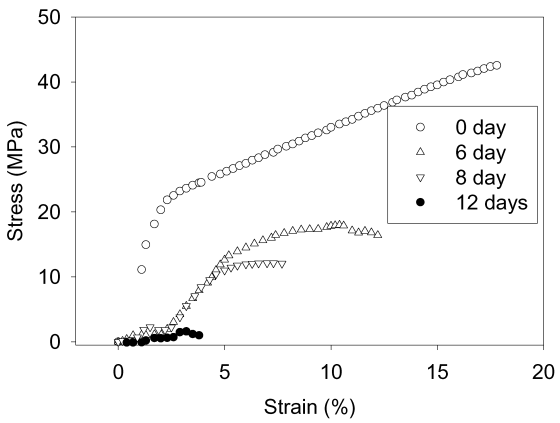

Fig. 9. Mechanical property changes of electrospun PLA10GA90 annealed at 90 °C at a constant strain of 450% during in vitro degradation of different times.

plasticization of the degraded products to the bulk polymer. The initial moduli of the stress–strain curves after the plastic flow zone were found to decrease with increasing degradation time. The membranes were found to gradually lose their tensile strength as well as the maximum strain at break at the later stages of degradation. The membrane became very weak and brittle after eight days of degradation.

Fig. 10 shows the degradation rate of the as-prepared PLA10GA90 membrane and the post-treated membrane (annealed at 90 °C for 20 min under a strain of 300%). The degradation rate of the post-treated membrane was slower in the beginning of incubation. This can be understood by the following explanation. It is well known that the degradation of PLGA polymers starts with the diffusion of water into the polymer matrix. It is more difficult for water to penetrate into the polymer matrix with a high degree of crystallinity. Therefore, the increase in crystallinity of the post-treated membrane retarded the diffusion rate of water into the membrane, which in turn decreased the degradation rate during the initial period. However, the amorphous chains in the un-treated PLA10GA90 membrane could also form a crystalline structure by thermal- and degradation-induced crystallization processes during incubation [25]. In the initial degradation stages, the formed crystalline structures in the un-treated PLA10GA90 membrane were defective, and thus were more susceptive to be attacked by water. It was interesting to note that the post-treated membrane after 14 days of incubation exhibited a faster rate than the un-treated PLA10GA90 membrane. This was probably due to the auto-catalyzed hydrolysis of PLA10GA90 polymer chains in the post-treated membrane. It was conceivable that once the crystalline region started to degrade in the post-treated membranes, oligomers would be formed and could be entrapped inside the denser microstructures of the polymer matrix. The accumulation of the oligomers with acid ending-groups could accelerate the hydrolysis reaction of the post-treated membranes.

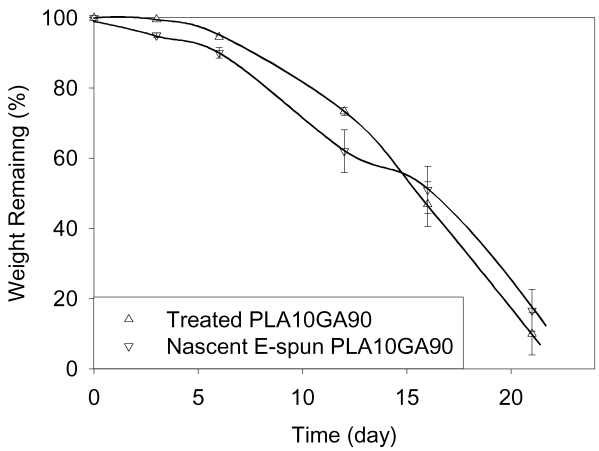

Fig. 10. in vitro weight loss of nascent electrospun PLA10GA90 membrane and membrane annealed at 90 °C for 20 min under the deformation strain of 300%.

4. Conclusions

Several major conclusions were made in this study, which are summarized as follows.

(1) The concentration changes of PLA10GA90 solution in HFIP not only affected the morphology and the microstructure formed during electrospinning, but also the mechanical properties. Higher concentrations favored the formation of pure fiber morphology with a low degree of crystallinity, which exhibited a higher value of tensile strength but a lower value of elongation at break.
(2) From X-ray results, it was found that the electrospun membranes crystallized at 90 °C under elongation showed an oriented crystalline lamellar structure. The crystallization process of electrospun PLA10GA90 membranes was significantly enhanced by tensile stretching. Higher crystal orientation was formed with the increase in tensile strain, whereas the temperature had a reverse effect on the crystal orientation.
(3) The tensile strength of the electrospun membranes was greatly improved by post-treatments (stretching and annealing). The tensile retention time for the membranes annealed under a strain of 300% at 90 °C for 20 min increased from 2 to 12 days during in vitro degradation. The post-treated membranes exhibited a slower degradation rate at the beginning of incubation, but a faster rate after two weeks of degradation.

Acknowledgements

Financial support of this work was provided by the Center for Biotechnology at Stony Brook, a National Institutes of Health-SBIR grant (GM63283-02) administered by the Stonybrook Technology and Applied Research, Inc., the SUNY-SPIR program and the US Department of Energy (DEFG 0299ER45760 and DEFG0286ER45237.017).

References

[1] Engelberg I, Kohn J. Biomaterials 1991;12:292–304.
[2] Chu CC. J Appl Polym Sci 1981;26:1727–34.
[3] Li S. J Biomed Mater Res 1999;48:342–53.
[4] Lu L, Garcia GA, Mikos AG. J Biomed Mater Res 1999;46:236–44.
[5] Lu L, Peter SJ, Lyman MD, Lai HL, Leite SM, Tamada JA, Uyama S, Vacanti JP, Langer R, Mikos AG. Biomaterials 2000;21:1837–45.
[6] King E, Cameron RE. J Appl Polym Sci 1997;66:1681–90.
[7] Fredericks RJ, Melveger AJ, Dolegiewitz LJ. J Polym Sci: Polym Phys Ed 1984;22:57–66.
[8] Ginde RM, Gupta RK. J Appl Polym Sci 1987;33:2411–29.
[9] Tsuji H, Ikada Y. J Appl Polym Sci 1997;63:855–63.
[10] Okuzaki H, Kubota I, Kunugi T. J Polym Sci B: Polym Phys 1999;37:991–6.

[11] Lee JK, Lee KH, Jin BS. Eur Polym J 2001;37:907–14.
[12] Andriano KP, Pohjonent T, Torrmala P. J Appl Biomater 1994;5: 133–40.
[13] Fang X, Reneker DH. J Macromol Sci Phys 1997;B36(2):169–73.
[14] Buchko CJ, Chen LC, Shen Y, Martin DC. Polymer 1999;40: 7397–407.
[15] Huang L, McMillan RA, Apkarian RP, Pourdeyhimi B, Conticello VP, Chaikof EL. Macromolecules 2000;33(8):2989–97.
[16] Boland ED, Wnek GE, Simpson DG, Pawlowski FJ, Bowlin GL. J Macromol Sci 2001;38:1231–43.
[17] Zong XH, Kim KS, Fang DF, Ran SF, Hsiao BS, Chu B. Polymer 2002;16:4403–12.
[18] Megelski S, Stephens JS, Chase DB, Rabolt JF. Macromolecules 2002;35:8456–66.
[19] Nagapudi K, Brinkman WT, Leisen JE, Huang L, McMillan RA, Apkarian RP, Conticello VP, Chaikof EL. Macromolecules 2002; 35(5):1730–7.
[20] Matthews JA, Wnek GE, Simpson DG, Bowlin GL. Biomacromolecules 2002;3:232–8.
[21] Li WJ, Laurencin CT, Caterson EJ, Tuan RS, Ko FK. J Biomed Mater Res 2001;60:613–21.
[22] Deitzel JM, Kleinmeyer JD, Hirvonen JK, Beck Tan NC. Polymer 2001;42(19):8163–70.
[23] Chatani Y, Suehiro K, Okita Y, Tadokoro H, Chujo K. Die Makromolekulare Chemie 1968;113:215–29.
[24] Ran S, Fang D, Zong X, Hsiao B, Chu B. Polymer 2001;42:1601–12.
[25] Zong XH, Ran SF, Kim KS, Fang DF, Hsiao BS, Chu B. Biomacromolecules 2003;4(2):416–23.